Medium Plant Cover has the Highest Heterogeneity of Fine-Scale Spatial Vegetation Patterns in Humid grasslands

Qin Yang
Guizhou University
Hua Cheng
Lanzhou University
Hongmei Pu
Guizhou University
Xuechun Zhao
Guizhou University
Rui Dong
Guizhou University
Yulian Chen
Guizhou University
Shenghui Yang
Guizhou University
X. Ben Wu
Texas A&M University College Station
Chao Chen
Guizhou University
Baocheng Jin (jinbch@outlook.com)
Guizhou University https://orcid.org/0000-0002-8973-9746

Research Article

Keywords: Landscape fragmentation, Landscape metrics, Patterned landscape, Scale, Shape index, Spatial heterogeneity

Posted Date: March 3rd, 2021

DOI: https://doi.org/10.21203/rs.3.rs-272768/v1

Abstract

Context Fine-scale spatial vegetation patterns are ubiquitous and can have profound impacts on large scale ecological processes including surface runoff, soil erosion, and livestock forage efficiency. However, we have limited knowledge of the fine-scale spatial vegetation patterns in humid grasslands.

Objectives The objectives were to characterize the spatial vegetation patterns at centimeter scale in humid grasslands, quantify the vegetation patterns variation under different image pixel sizes and plant covers, and explore the potential ecological implications of the spatial vegetation patterns.

Methods Seventy plots with plant covers ranging from 30.8–99.3% were selected from seven humid grasslands in southwest China and their spatial vegetation patterns quantified at image pixel sizes of 0.04, 0.25, 1, and 4 cm.

Results With increasing pixel size, plant patch density and total edge density decreased, plant patch size increased, and the plant patch shape became more regular. At a plant cover level below 50%, increasing plant cover will result in increasing patch density and patch size, leading to greater spatial heterogeneity. At plant cover levels above 50%, increasing plant cover will cause the rapid expansion of patch size, along with a lower patch density, forming a more homogeneous landscape dominated by plant patches. The small stems, branches, and leaves of grasses fragmented non-plant patches into smaller patches with increasing plant cover; this fragmentation resembles road-induced landscape fragmentation processes.

Conclusions Medium plant cover has the highest heterogeneity of spatial vegetation pattern at the fine scale, which may have significant implications on ecological processes and related management practices.

Introduction

Fine-scale spatial vegetation patterns are ubiquitous, and they can have profound impacts on larger scale ecological processes including surface runoff (Puigdefabregas 2005; Bautista et al. 2007; Sun et al. 2019), soil erosion (Lin et al. 2010; Zhang et al. 2011; Hou et al. 2016), and livestock forage efficiency (Jin et al. 2016). Quantifying fine-scale spatial vegetation patterns may therefore allow a deeper insight into these larger scale ecological processes, facilitating the development of adequate management practices.

Plant cover is a key factor affecting fine-scale spatial vegetation patterns. It is defined as the percentage of ground surface covered by vegetation (Greig-Smith 1983; Bonham et al. 2004; Bonham and Clark 2005; Fehmi 2010; Bonham 2013) is one of the most measured and fundamental characteristics of grassland ecosystems. In their study in a desert steppe in Inner Mongolia, China, Lin et al. (2010) found a positive linear relationship between plant cover and the total edge of plant patches. In contrast, in a study in a Mediterranean grassland with 600 mm of precipitation and approximately 50% woody plant cover, with a considerable herbaceous plant cover, Bar Massada et al. (2008) showed that increasing plant cover will

lead to fine-scale vegetation fragmentation and a decreased edge density. These authors also observed a similar mean shape index (a measure of patch shape complexity) for treatments with different plant covers (Bar Massada et al. 2008). In the above-mentioned studies, the plant cover was low or medium (Bar Massada et al. 2008; Lin et al. 2010). To clarify the relationship between spatial vegetation pattern and plant cover, it is important to involve more sampling plots with medium and high plant cover.

Image pixel size is another important factor affecting fine-scale spatial vegetation patterns. Previous studies at larger scales found that changing image pixel sizes had significant effects on the values of landscape metrics (Wu et al. 2002; Wu 2004; Gustafson, 2019). For example, at large scales, patch density, shape index, and patch size coefficient of variation decreased, but patch size increased with increasing pixel sizes from 30 to 3,000 meters (Wu et al. 2002; Wu 2004). At finer scales, a study using 4-cm pixel images, acquired by low-altitude aerial balloon photography, could not separate bare ground and herbaceous vegetation in the dry season (Bar Massada et al. 2008). Another fine-scale research conducted in a desert steppe using 2-cm pixel images found that the largest patch index and coefficient of variation of the mean patch area was negatively linearly related with grazing intensity (Lin et al. 2010). At the scale of about 1 mm pixel size, Hou et al. (2016) found a negative correlation between the landscape shape index and the plant cover of grasslands of the Qinghai-Tibet Plateau. To adequately characterize and monitor spatial vegetation patterns, multiscale analysis is a useful tool (Wu et al. 2002; Wu 2004). However, multiscale studies at the centimeter scale are scarce (but see Bar Massada et al. 2008).

In this context, the objectives of this study were to (1) characterize the spatial vegetation patterns at centimeter scale in humid grasslands of southwest China, (2) quantify the vegetation patterns variation under different image pixel sizes and plant covers, and (3) explore the possible ecological implications of the fine-scale spatial vegetation patterns.

Methods

Study area

In Guizhou Province of southwest China (24°37’–29°13’N, 103°36’–109°35’E; 150–2,900 m elevation; Fig. 1a); we established 70 plots in 7 sites (with 10 plots per site), namely in Zhuopu, Jiucaiping, Wumeng, Youshanhe, Maiping, Yunding, and Xujiaba. The climate is humid subtropical monsoon climate, with a mean (1981–2010) annual temperature of 14.2°C and a mean annual precipitation of 1,069.9 mm (Fig. 1b and 1c). The mean daily temperatures of the coldest (January) and warmest (July) months were 4.4 and 22.2°C, respectively (Fig. 1b, data from the China Meteorological Data Center; https://data.cma.cn/). The elevation of the plots ranges between 920.0 and 2,698.0, with an average of 1,874.1 m. The common slope gradient of the plots ranges between 0.3 and 9.5°, with an average of 3.1°. According to the FAO 90 taxonomy (FAO 2012), the soils are Haplic Alisols (Youshanhe, Maiping, Xujiaba), Haplic Luvisols (Zhuopu and Jiucaiping), and Dystric Regosols (Wumeng and Yunding). The vegetation is composed of *Trifolium repens, Lolium perenne, Paspalum thunbergii, Dactylis glomerata,*

Arthraxon hispidus, Bothriochloa ischaemum, Plantago depressa, Festuca rubra, Eragrostis pilosa, Potentilla chinensis, and *Miscanthus floridulus*. The study sites have been used for light or medium grazing and rural tourism for more than 10 years.

Sampling and analyses

Field sampling was conducted near the local peak biomass season (July to September) to characterize the spatial vegetation patterns, the plant community, and the soil characteristics. A photograph of each sampling plot (1m × 1m in size) was taken at the angle perpendicular to the horizontal plane, using a 16-million-pixel common digital camera. The photo image was then classified into plant or non-plant pixels using supervised classification via ERDAS IMAGINE (version 2013, ERDAS, USA). The accuracy of the classification was 94.9 ± 2.9% (mean ± std, n = 70), based on comparison with independent visual interpretation at 102 randomly selected points within each plot. Pixel size ranged between 0.03 and 0.06 cm (0.04 ± 0.01 cm), depending on camera height (approximately 2 m) and plant height (2.3–34.3 cm, 14.6 ± 9.0 cm). The original photo images (approximately 0.04 cm pixel size) were rescaled to three coarser scales, with pixel sizes of 0.25, 1, and 4 cm (Fig. 2). The plant and non-plant spatial distribution patterns were calculated at patch, class, and landscape levels, based on the classified images, using the Fragstats v. 4.2 software (McGarigal et al. 2012).

The height of each species was recorded in the field. The plants in each plot were collected by species, dried for 48 h at 65°C, and weighted to determine aboveground plant biomass. Soil samples were collected at a depth of 0–10 cm perpendicular to the horizontal plane. Two soil cores were extracted using a 5-cm diameter soil auger. One core (about 100 g) was weighted, dried for 48 h at 105°C, and reweighted to determinate soil bulk density. Another soil core was washed through a sieve (0.074 mm) to collect plant roots, which were dried for 48 h at 65°C and then weighted to determine belowground plant biomass. We used one-way ANOVA to determine differences among the plots for the relevant variables, using the software package SPSS (version 10.0, IBM, USA).

Results

At a pixel size of approximately 0.04 cm, there were 467.1 ± 716.7 plant patches within each sampling plot (1 × 1m in size). Patch density decreased with increasing pixel size. At pixel sizes of 0.25, 1, and 4 cm, there were 301.6 ± 472.2, 35.5 ± 72.2, and 3.4 ± 6.3 plant patches. At 0.04 cm, the percentages of plant patches within patch sizes of 0–10 cm^2, 10–100 cm^2, 100–1,000 cm^2, and 1,000–10,000 cm^2 were 85.2 ± 23.1%, 0.4 ± 0.5%, 0.0 ± 0.1%, and 14.4 ± 23.3% (Fig. 3a), covering 1.8 ± 0.1%, 7.3 ± 1.6%, 19.2 ± 3.3%, and 51.2 ± 21.6% of the occupied area, respectively (Fig. 3b). With increasing pixel size, the percentage of small plant patches decreased, but the percentage of medium and large patches increased gradually (Fig. 3a). The patch area percent distribution patterns were similar for different pixel sizes (Fig. 3b).

Plant cover ranged from 30.8–99.3%, and patch density declined with increasing plant cover (Fig. 4a). There was a trend of quadratic regression between plant cover and edge density (Fig. 4b), patch area

variable coefficient (Fig. 4e), and shape index (Fig. 4f); the corresponding plant cover for the maximum curve value was approximately 50%. Mean patch area (Fig. 3c) and gyration radius (Fig. 3d) increased nearly exponentially with increasing plant cover.

For plant patches, with increasing plant cover, except for the largest patch size interval (1,000–10,000 cm^2), patch density decreased for all patch size intervals (0–10 cm^2, 10–100 cm^2, 100–1000 cm^2) and pixel sizes (0.04, 0.25, 1, 4 cm) (Fig. 5a-c). However, large patches declined to zero faster than small patches (Fig. 5a-c). When the plant cover was approximately 90, 73, and 67%, plant patch density decreased to zero for patch size intervals of 0–10 cm^2, 10–100 cm^2, and 100–1000 cm^2, respectively (Fig. 5a-c). When the plant cover was approximately 40%, the plant patch density for the largest patch size interval (1,000–10,000 cm^2) increased from zero to one (Fig. 5d).

For non-plant patches, with increasing plant cover, except for the largest patch size interval (1,000–10,000 cm^2), patch density showed obvious quadratic polynomial regression patterns (Fig. 5e-g). The corresponding plant cover for the maximum values of the curves was consistently smaller for large patch size intervals (Fig. 5e-g). At plant cover levels of 82–90%, 60–83%, and 61–68%, non-plant patch density peaked for patch size intervals of 0–10 cm^2, 10–100 cm^2, and 100–1,000 cm^2, respectively (Fig. 5e-g). When the plant cover was approximately 54–66%, non-plant patch density for the largest patch size interval (1,000–10,000 cm^2) decreased from 1 to 0 count/m^2 (Fig. 5h).

For both plant and non-plant patches, the largest patch index (the percentage of the landscape comprised by the largest patch, LPI) was dependent on plant cover (Fig. 6). However, the largest patch index of plant patches increased with increasing plant cover, but that of non-plant patches decreased with increasing plant cover (Fig. 6). The intersection point of the two fit curves was 47.7% plant cover (Fig. 6).

We found a quadratic polynomial regression between landscape division index and plant cover (Fig. 7a). The corresponding plant cover for the maximum value of the curve was 52%, indicating that the landscape is maximally subdivided under medium plant cover (Fig. 7a). The Contagion index declined to its lowest point when the plant cover was 51.6% (Fig. 7b), indicating the highest level of interspersion of plant and non-plant patches.

We found no statistically significant differences in plant cover and species number among sampling plots dominated by plants of different families (Fig. 8a, 8c). *Leguminosae* plant communities (6.5 ± 3.3 cm, 19 sampling plots) were shorter than *Poaceae* plant communities (18.1 ± 8.4 cm, 46 sampling plots), and mixed (*Leguminosae* and *Poaceae*, 5 sampling plots) plant communities (12.5 ± 9.7 cm) were intermediate (Fig. 8b). Aboveground biomass was highest for *Poaceae* (231.8 ± 86.6 g/m^2), followed by *Leguminosae* (136.7 ± 45.4 g/m^2) and mixed (*Leguminosae* and *Poaceae*) plant communities (113.7 ± 39.0 g/m^2; Fig. 8d). Belowground biomass was lowest for *Leguminosae* (45.5 ± 42.0 g/m^2), followed by *Poaceae* (437.8 ± 262.4 g/m^2) and mixed plant communities (463.0 ± 387.3 g/m^2, Fig. 8e). Soil bulk density was highest under *Leguminosae* plant communities (1.3 ± 0.3 g/cm^3), intermediate in *Poaceae* plant communities (1.1 ± 0.2 g/cm^3), and lowest in mixed plant communities (1.0 ± 0.1 g/cm^3, Fig. 8f).

For plant patches, at pixel sizes of 0.04 and 0.25 cm, patch amount and shape index were highest in mixed (*Leguminosae* and *Poaceae*), intermediate in *Poaceae*, and lowest in *Leguminosae* plant communities (Table 1). At pixel sizes of 1 and 4 cm, there was no statistically significant difference for both plant patch density and shape index (Table 1). For non-plant patch density, there was no statistically significant difference among sampling plots dominated by plants of different families (Table 1). Except at a pixel size of 4 cm, the non-plant shape index of mixed plant communities (*Leguminosae* and *Poaceae*) was higher than that of *Poaceae* and *Leguminosae* plant communities (Table 1).

Table 1
Patch density and shape index for sampling plots dominated by plants of different families. Different letters indicate significant differences at P = 0.05.

Plant/ Non-plant	Pixel size (cm)	Patch density (count/m^2)			Shape index		
		Leguminosae	*Poaceae*	Mixed	*Leguminosae*	*Poaceae*	Mixed
Plant	0.04	281.1 ± 305.0b	454.5 ± 739.3b	1290.2 ± 1131.2a	47.5 ± 14.7b	59.9 ± 40.2b	94.6 ± 30.9a
	0.25	160.8 ± 170.1b	323.4 ± 536.1ab	635.8 ± 493.6a	33.4 ± 10.7b	39.0 ± 26.7ab	57.8 ± 13.0a
	1	17.8 ± 23.9a	42.1 ± 86.4a	43.0 ± 36.5a	15.5 ± 6.0a	15.5 ± 10.5a	22.5 ± 4.4a
	4	1.8 ± 1.6a	4.1 ± 7.7a	2.8 ± 2.1a	5.0 ± 1.7a	4.7 ± 2.7a	6.9 ± 1.4a
Non-plant	0.04	4398.0 ± 1764.6a	4884.9 ± 2719.0a	5493.2 ± 2555.6a	90.6 ± 15.1b	108.7 ± 31.4ab	129.9 ± 29.8a
	0.25	2490.2 ± 860.4a	2722.7 ± 1433.2a	2627.0 ± 1244.3a	62.8 ± 8.1b	68.0 ± 17.8ab	79.6 ± 12.6a
	1	422.7 ± 119.9a	336.2 ± 198.5a	295.2 ± 142.0a	27.6 ± 2.9a	25.3 ± 7.4a	30.4 ± 1.5a
	4	36.6 ± 10.9a	26.3 ± 17.3a	29.8 ± 14.0a	8.0 ± 1.1ab	6.8 ± 2.3b	9.1 ± 0.4a

Discussion

Spatial vegetation patterns under different image pixel sizes

Multiscale analysis can be applied to adequately characterize and monitor spatial vegetation patterns (Wu et al. 2002; Wu 2004). Here, spatial vegetation patterns of humid grasslands were quantified at image pixel sizes of 0.04 (original photo image), 0.25, 1, and 4 cm, using camera photography. Changing

pixel size had important effects on most landscape metrics. The plant patch density and the total edge density decreased, whereas the patch size increased and the plant patch shape became more regular with increasing pixel size. This result was consistent with previous studies about the effects of changing scales on landscape metrics (Wu et al. 2002; Wu 2004; Gustafson 2019).

Based on our results, the most adequate pixel size for the analysis of fine-scale spatial vegetation patterns is less than 0.25 cm, which is considerably smaller than those used in previous studies (Wu et al. 2000; Maestre et al. 2005; Lin et al. 2010; Hou et al. 2016). In a previous study, using 4-cm pixel images obtained via low-altitude aerial balloon photography, the authors could not separate bare ground from herbaceous vegetation in the dry season (Bar Massada et al. 2008). Another study, using images with a pixel size of 2 cm, acquired with a digital camera, may have ignored considerable detailed plant distribution information (Lin et al. 2010). In this study, the original photos (approximately 0.04 cm pixel size) were rescaled to three coarser scales, with pixel sizes ranging from approximately 0.04 to 4 cm. There were similar plant patch densities (467.1 versus 301.6 count/m^2) and edge density levels (1.9 versus 1.2 cm/cm^2), patch area mean (1,387.3 versus 1,355.2 cm^2), and radius levels of gyration (30.7 versus 20.3 cm) for pixel sizes of 0.04 and 0.25 cm. However, these landscape metrics decreased or increased dramatically when pixel sizes were increased from 0.25 to 4 cm, indicating a rapid loss of information. In addition, our visual interpretation showed that the pixel size required to distinguish small stems, branches, and leaves was close to 0.25 cm.

The centimeter-scale spatial vegetation pattern may be an essential part of patterned landscapes, forming a hierarchical view from scales of centimeters to 1,000 meters. The fine scale of the spatial vegetation pattern was considerably smaller than that of banded landscapes composed of alternating bands of vegetation and bare ground in arid and semi-arid regions (Valentin and d'Herbes 1999; Deblauwe et al. 2012), shrub patches (Zhang et al. 2011; Bhattachan et al. 2014), and networks of livestock tracks on hilly rangelands (Stavi et al. 2008; Jin et al. 2016). There were different formation mechanisms, and the banded landscapes were derived from eco-hydrological processes and water redistribution from non-vegetated to vegetated areas (Valentin and d'Herbes 1999; Saco et al. 2007). The terraced landscapes are a result of track formation by livestock (Howard and Higgins 1987; Jin et al. 2019). The shrub patches and the fine-scale spatial vegetation patterns originated from plant growth.

Medium plant cover has the highest heterogeneity of spatial vegetation pattern at the fine scale

Plant cover acts as another key factor affecting fine-scale spatial vegetation patterns. Medium plant cover may have the greatest spatial heterogeneity of fine-scale vegetation distribution in humid grasslands of southwest China. This hypothesis is based on the findings of this and other studies. First, when the plant cover was higher or close to 50%, there was a negative correlation between plant cover and patch density, edge density, and shape index. Second, at a plant cover level of approximately 50%, the patch area variable coefficient reached the maximum. Third, there was a trend of quadratic regression between landscape division index and plant cover, peaking at about 50%, indicating that the landscape is maximally subdivided under medium plant cover. Forth, when the plant cover level was approximately

50%, the contagion index was lowest, indicating the highest level of interspersion of plant and non-plant patches. This hypothesis is also consistent with previous research conducted in a desert steppe in Inner Mongolia, China, and showing that the total edge of plant patches increased with increasing plant cover (Lin et al. 2010). In contrast, in a study conducted in a Mediterranean grassland with 600 mm precipitation, approximately 50% woody plant cover, and a considerable herbaceous plant cover, increasing plant cover led to fine-scale vegetation fragmentation and a decreased edge density (Bar Massada et al. 2008). Previous studies also found a weak quadratic regression between shape index and plant cover, although their plant cover levels were medium (Bar Massada et al. 2008; Hou et al. 2016). We speculate that at a plant cover level below 50%, the landscape is mainly composed of non-plant patches, with sufficient space for plant growth. In such areas, increasing plant cover will result in increasing patch density and patch size, leading to greater spatial heterogeneity. In contrast to low plant cover, at cover levels above 50%, the landscape was mainly composed of plant patches, and increasing plant cover will cause a rapid expansion of patch size (caused by the growth of already existing stems, branches, and leaves), but also a decrease in patch density (caused by the interconnection of plant patches), forming a homogeneous landscape dominated by plant patches. The highest heterogeneity of spatial vegetation patterns, at medium plant cover, may have potential positive ecological implication at the fine scale (Webster et al. 2002; Schindler et al. 2013; Stein et al. 2014; Manlick et al. 2020).

Increasing plant cover leads to fine-scale non-plant patch fragmentation

With increasing plant cover, except for the largest patch size interval (1,000–10,000 cm^2), non-plant patch density within different patch size intervals (0–10 cm^2, 10–100 cm^2, and 100–1,000 cm^2) increased first and then decreased, and larger patch size intervals reached their highest points earlier. This leads us to infer that the small stems, branches, and leaves of grasses fragmented non-plant patches into smaller patches with increasing plant cover. The plots dominated by gramineous plants (mostly *Lolium perenne* and *Paspalum thunbergii*) with long and narrow leaves could fragment the non-plant patches more efficiently (namely more small non-plant patches) than plots dominated by *Trifolium repens*, with oval or elliptical small leaves, although the plant cover levels were similar. This fine-scale non-plant patch fragmentation resembles road-induced landscape fragmentation processes, dissecting the non-plant landscape, leading to non-plant landscape fragmentation, shrinkage, and attrition at a large scale (Saunders et al. 2002; Forman et al. 2003; Hawbaker et al. 2006; Fahrig 2019).

Conclusions

Changing pixel size had important effects on most landscape metrics. With increasing pixel size, plant patch density and total edge density decreased and plant patch size increased; plant patch shape became more regular. The adequate pixel size for the analysis of the fine-scale spatial vegetation patterns is less than 0.25 cm. The centimeter-scale spatial vegetation pattern may be an essential part of patterned landscapes, forming a hierarchical view from scales of centimeters to 1,000 meters. Plant cover acts as another key factor affecting fine-scale spatial vegetation patterns. Medium plant cover had the greatest spatial heterogeneity of fine-scale vegetation distribution. At a plant cover level below 50%, the

landscape was mainly composed of non-plant patches, with sufficient space for plant growth. Increasing plant cover will result in increasing patch density and patch size, leading to greater spatial heterogeneity. In contrast, at plant cover levels above 50%, the landscape was mainly composed of plant patches. Increasing plant cover will cause rapid patch size expansion, but also a lower patch density, forming a more homogeneous landscape dominated by plant patches. Grass blades fragmented non-plant patches into smaller patches with increasing plant cover. In this sense, increasing plant cover leads to fine-scale non-plant patch fragmentation. Based on our results and on the findings of previous studies, spatial vegetation patterns, jointly affected by image pixel size and plant cover in humid grasslands, may have significant implications on ecological processes and related management practices, albeit at a fine scale.

Declarations

Acknowledgements

We thank Zhengxue Zhao, Biyou Shu, Hongsong Zhang, Jiaai Li, Xiaobing Chen, Lukun Li, Bo Ding, and Dengming He for assistance with field work. This work was partially supported by grants to BJ from the National Natural Science Foundation of China (31700390), a grant to XZ (Qian Ke He Zhicheng[2020]1Y076) from the Science and Technology Department of Guizhou Province, grants to RD from the National Natural Science Foundation of China (32060392) and Science and Technology Department of Guizhou Province (Qian Ke He Jichu[2019]1074 and Qian Ke He Zhicheng[2020]1Y074), and CC (RCJD2018-13, GZZ2017001, Qian Ke He Zhicheng[2018]2258) from the Science and Technology Department of Guizhou Province.

References

1. Bar Massada A, Gabay O, Perevolotsky A, Carmel Y (2008) Quantifying the effect of grazing and shrub-clearing on small scale spatial pattern of vegetation. Landsc Ecol 23:327–339. https://doi.org/10.1007/s10980-007-9189-0
2. Bautista S, Mayor AG, Bourakhouadar J, Bellot J (2007) Plant spatial pattern predicts hillslope runoff and erosion in a semiarid Mediterranean landscape. Ecosystems 10:987–998. https://doi.org/10.1007/s10021-007-9074-3
3. Bhattachan A, D'Odorico P, Dintwe K, Okin GS, Collins SL (2014) Resilience and recovery potential of duneland vegetation in the southern Kalahari. Ecosphere 5:art2. https://doi.org/10.1890/ES13-00268.1
4. Bonham CD (2013) Measurements for Terrestrial Vegetation, second edn. John Wiley & Sons, New York
5. Bonham CD, Clark DL (2005) Quantification of plant cover estimates. Grassl Sci 51:129–137. https://doi.org/10.1111/j.1744-697X.2005.00018.x
6. Bonham CD, Mergen DE, Montoya S (2004) Plant cover estimation: a contiguous Daubenmire frame. Rangelands 26:17–22. https://doi.org/10.2458/azu_rangelands_v26i1_bonham 16.

7. Deblauwe V, Couteron P, Bogaert J, Barbier N (2012) Determinants and dynamics of banded vegetation pattern migration in arid climates. Ecol Monogr 82:3–21. https://doi.org/10.5061/dryad.1qr41s56
8. Fahrig L (2019) Habitat fragmentation: A long and tangled tale. Glob Ecol Biogeogr 28:33–41. https://doi.org/10.1111/geb.12839
9. FAO I ISRIC, ISSCAS JRC (2012) Harmonized world soil database (version 1.2). FAO, Rome, Italy and IIASA, Laxenburg, Austria
10. Fehmi JS (2010) Confusion among three common plant cover definitions may result in data unsuited for comparison. J Veg Sci 21:73–279. https://doi.org/10.1111/j.1654-1103.2009.01141.x
11. Fick SE, Hijmans RJ (2017) WorldClim 2: new 1-km spatial resolution climate surfaces for global land areas. Int J Climatol 37:4302–4315. https://doi.org/10.1002/joc.5086
12. Forman RT, Sperling D, Bissonette JA, Clevenger AP, Cutshall CD, Dale VH, Fahrig L, Heanue K, France RL, Goldman CR (2003) Road Ecology: Science and Solutions. Island Press, Washington, DC
13. Greig-Smith P (1983) Quantitative Plant Ecology. University of California Press, California
14. Gustafson EJ (2019) How has the state-of-the-art for quantification of landscape pattern advanced in the twenty-first century? Landsc Ecol 34:2065–2072. https://doi.org/10.1007/s10980-018-0709-x
15. Hawbaker TJ, Radeloff VC, Clayton MK, Hammer RB, Gonzalez-Abraham CE (2006) Road development, housing growth, and landscape fragmentation in northern Wisconsin: 1937–1999. Ecol Appl 16:1222–1237. https://doi.org/10.1890/1051-0761(2006)016[1222:RDHGAL]2.0.CO;2
16. Hou J, Wang H, Fu B, Zhu L, Wang Y, Li Z (2016) Effects of plant diversity on soil erosion for different vegetation patterns. Catena 147:632–637. https://doi.org/10.1016/j.catena.2016.08.019
17. Howard JK, Higgins CG (1987) Dimensions of grazing-step terracettes and their significance. In: Gardiner V (ed) International Geomorphology 1986 Part II. John Wiley & Sons, Chichester, pp 545–568
18. Jin B, Sun G, Cheng H, Zhang Y, Zou M, Ni X, Luo K, Zhang X, Li F, Wu XB (2019) Goat track networks facilitate efficiency in movement and foraging. Landsc Ecol 34:2033–2044. https://doi.org/10.1007/s10980-019-00877-w
19. Jin B, Sun G, Zhang Y, Zou M, Ni X, Luo K, Zhang X, Cheng H, Li F, Wu XB (2016) Livestock tracks transform resource distribution on terracette landscapes of the Loess Plateau. Ecosphere 7:e01337. https://doi.org/10.1002/ecs2.1337
20. Lin Y, Han G, Zhao M, Chang SX (2010) Spatial vegetation patterns as early signs of desertification: a case study of a desert steppe in Inner Mongolia, China. Landsc Ecol 25:1519–1527. https://doi.org/10.1007/s10980-010-9520-z
21. Maestre FT, Rodriguez F, Bautista S, Cortina J, Bellot J (2005) Spatial associations and patterns of perennial vegetation in a semi-arid steppe: a multivariate geostatistics approach. Plant Ecol 179:133–147. https://doi.org/10.1007/s11258-004-4641-6

22. Manlick PJ, Windels SK, Woodford JE, Pauli JN (2020) Can landscape heterogeneity promote carnivore coexistence in human-dominated landscapes? Landsc Ecol 35:2013–2027. https://doi.org/10.1007/s10980-020-01077-7
23. McGarigal K, Cushman SA, Ene E (2012) FRAGSTATS v4: spatial pattern analysis program for categorical and continuous maps. Computer software program produced by the authors at the University of Massachusetts, Amherst
24. Puigdefabregas J (2005) The role of vegetation patterns in structuring runoff and sediment fluxes in drylands. Earth Surf Process Landf 30:133–147. https://doi.org/10.1002/esp.1181
25. Saco PM, Willgoose GR, Hancock GR (2007) Eco-geomorphology of banded vegetation patterns in arid and semi-arid regions. Hydrol Earth Syst Sci 11:1717–1730. https://doi.org/10.5194/hess-11-1717-2007
26. Saunders SC, Mo RM, Chen J, Cleland DT (2002) Effects of roads on landscape structure within nested ecological units of the Northern Great Lakes Region, USA. Biol Conserv 103:09–225. https://doi.org/10.1016/S0006-3207(01)00130-6
27. Schindler S, von Wehrden H, Poirazidis K, Wrbka T, Kati V (2013) Multiscale performance of landscape metrics as indicators of species richness of plants, insects and vertebrates. Ecol Indic 31:41–48. https://doi.org/10.1016/j.ecolind.2012.04.012
28. Stavi I, Ungar ED, Lavee H, Sarah P (2008) Grazing-induced spatial variability of soil bulk density and content of moisture, organic carbon and calcium carbonate in a semi-arid rangeland. Catena 75:288–296. https://doi.org/10.1016/j.catena.2008.07.007
29. Stein A, Gerstner K, Kreft H (2014) Environmental heterogeneity as a universal driver of species richness across taxa, biomes and spatial scales. Ecol Lett 17:866–880. https://doi.org/10.1111/ele.12277
30. Sun W, Mu X, Gao P, Zhao G, Li J, Zhang Y, Chiew F (2019) Landscape patches influencing hillslope erosion processes and flow hydrodynamics. Geoderma 353:391–400. https://doi.org/10.1016/j.geoderma.2019.07.003
31. Valentin C, d'Herbes JM (1999) Niger tiger bush as a natural water harvesting system. Catena 37:231–256. https://doi.org/10.1016/s0341-8162(98)00061-7
32. Webster G, Embley TM, Prosser JI (2002) Grassland management regimens reduce small-scale heterogeneity and species diversity of beta-proteobacterial ammonia pxidizer populations. Appl Environ Microbiol 68:0–30. https://doi.org/10.1128/aem.68.1.20-30.2002
33. Wu J (2004) Effects of changing scale on landscape pattern analysis: scaling relations. Landsc Ecol 19:125–138. https://doi.org/10.1023/B:LAND.0000021711.40074.ae
34. Wu J, Shen W, Sun W, Tueller PT (2002) Empirical patterns of the effects of changing scale on landscape metrics. Landsc Ecol 17:761–782. https://doi.org/10.1023/A:1022995922992
35. Wu XB, Thurow TL, Whisenant SG (2000) Fragmentation and changes in hydrologic function of tiger bush landscapes, south-west Niger. J Ecol 88:790–800. https://doi.org/10.1046/j.1365-2745.2000.00491.x

36. Zhang P, Yang J, Zhao L, Bao S, Song B (2011) Effect of *Caragana tibetica* nebkhas on sand entrapment and fertile islands in steppe-desert ecotones on the Inner Mongolia Plateau, China. Plant Soil 347:79–90. https://doi.org/10.1007/s11104-011-0813-z

Figures

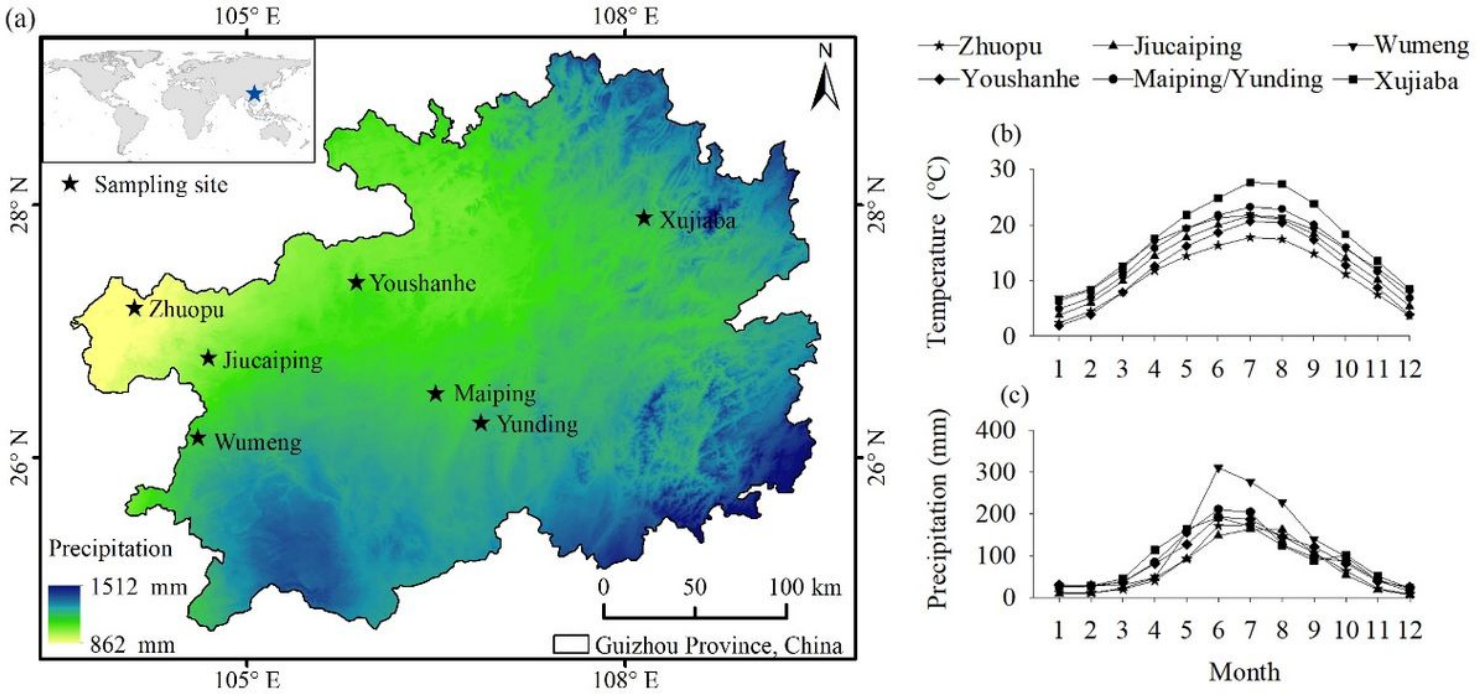

Figure 1

Location of the sampling sites and their monthly temperature and precipitation values. Temperature and precipitation data were derived from the China Meteorological Data Center (https://data.cma.cn/). The 30-second (~1 km2) spatial resolution precipitation data were derived from the WorldClim 2.1 dataset (Fick and Hijmans 2017). Note: The designations employed and the presentation of the material on this map do not imply the expression of any opinion whatsoever on the part of Research Square concerning the legal status of any country, territory, city or area or of its authorities, or concerning the delimitation of its frontiers or boundaries. This map has been provided by the authors.

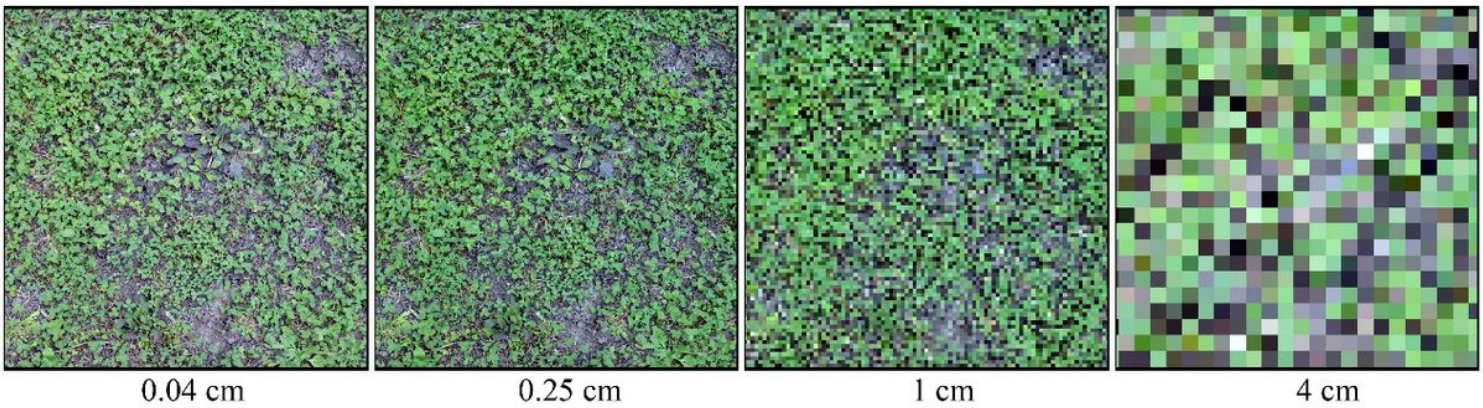

Figure 2

Example of an original photo image and its rescaled images with pixel sizes of 0.25, 1, and 4 cm.

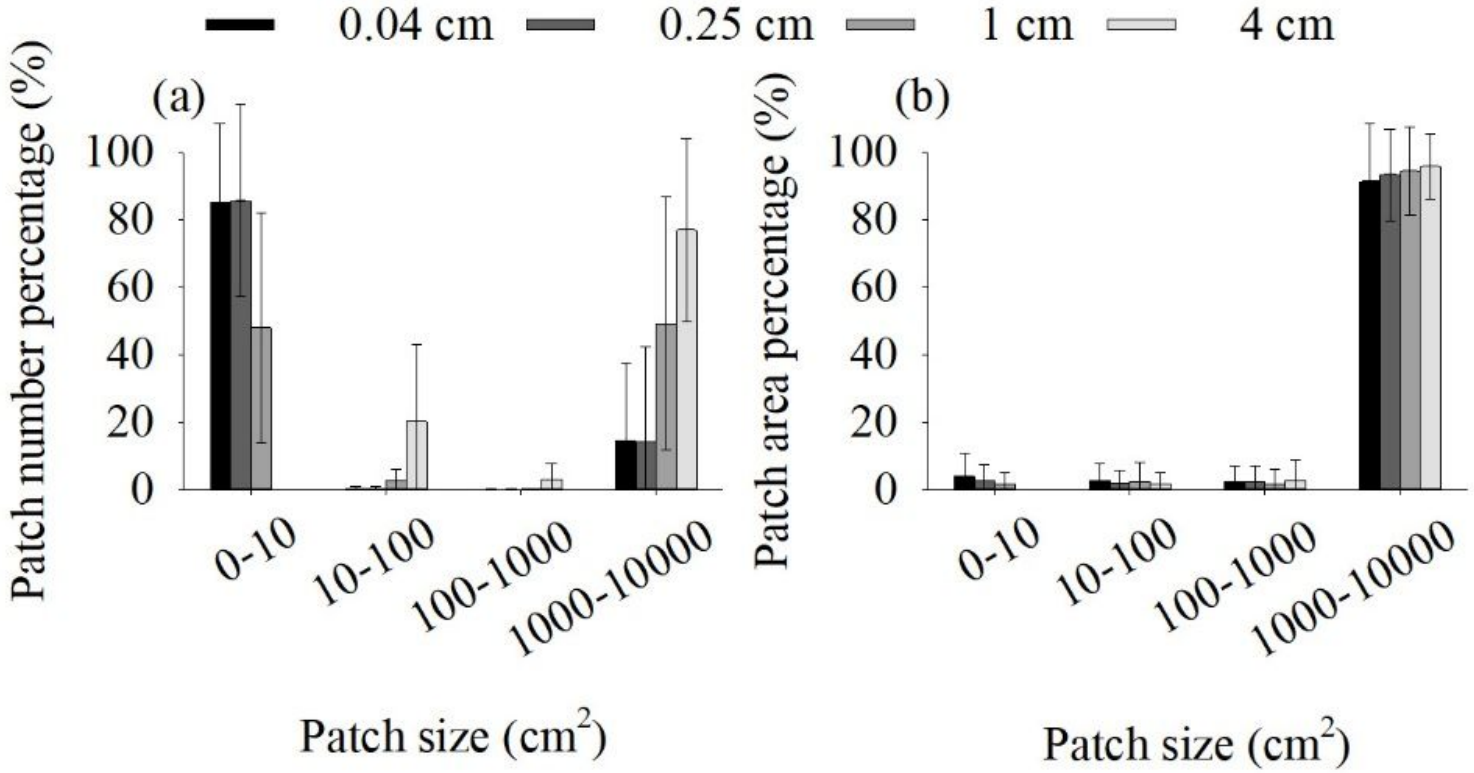

Figure 3

Patch number and area percentage distribution.

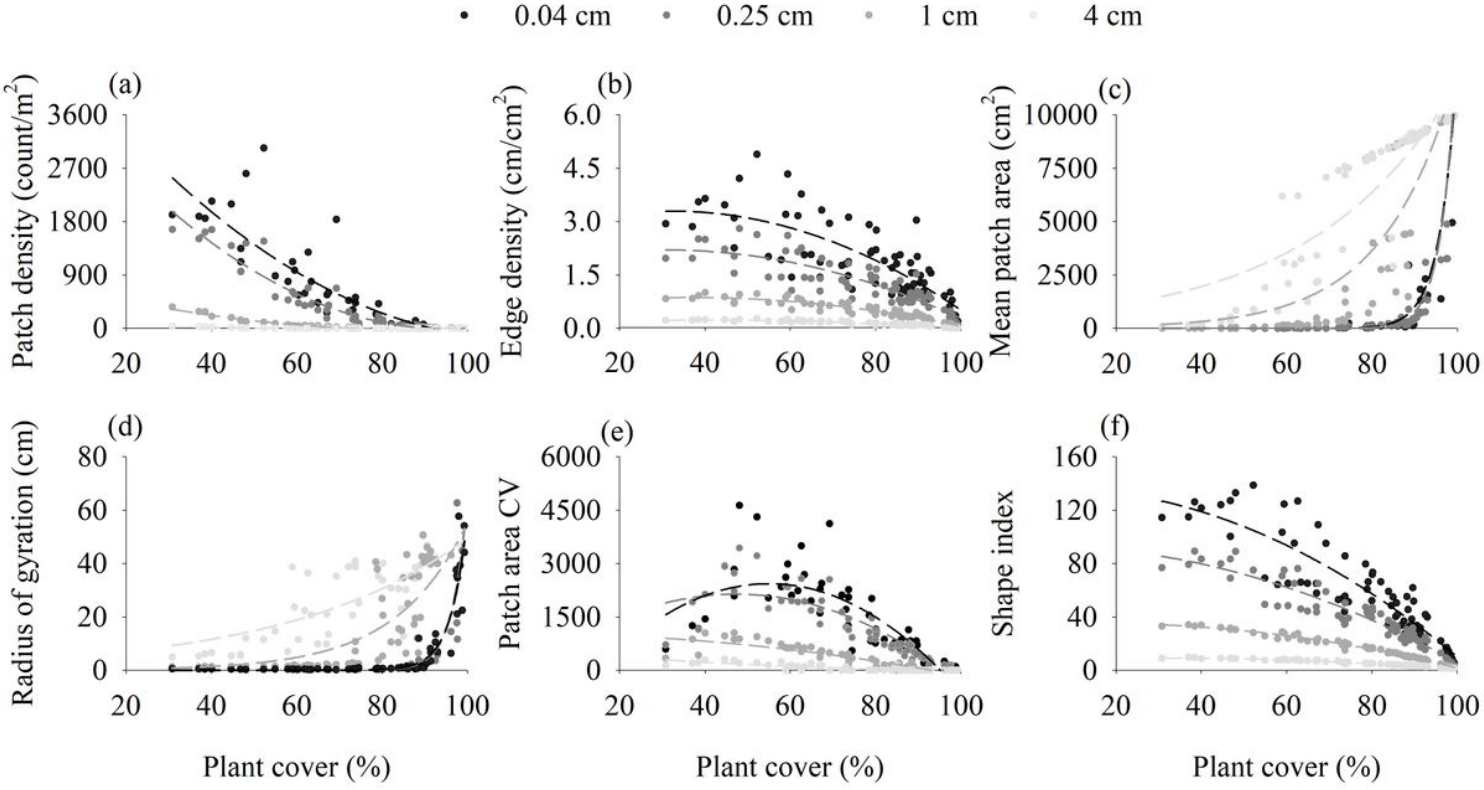

Figure 4

Patch density, edge density, mean patch area, gyration radius, patch area variable coefficient, and shape index for plots with different plant cover levels.

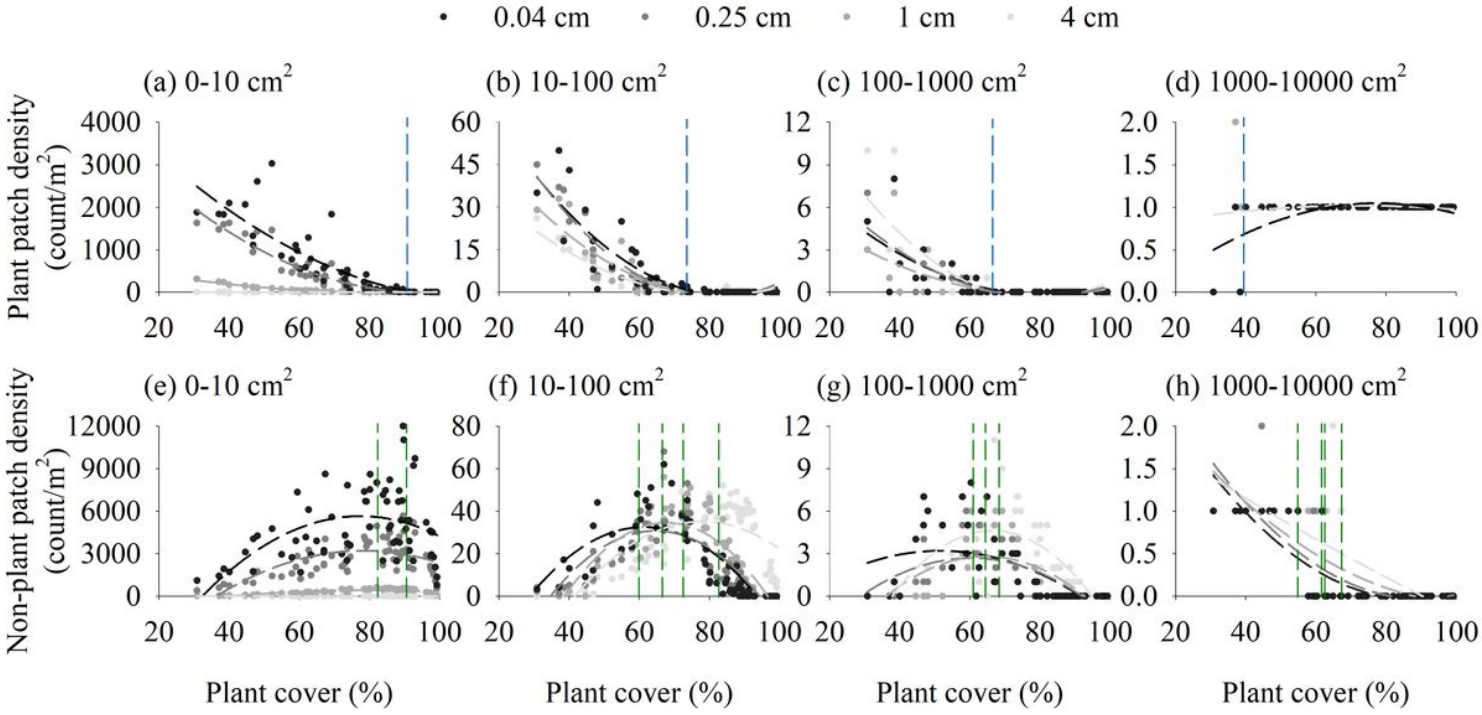

Figure 5

Plant and non-plant patch densities for different patch size intervals and pixel sizes under different plant covers. The blue lines within figures a-c indicate the transition points when patch density declined to 0 count/m2. The blue line within figure d indicates the transition point from zero to one. The green lines within figures e-g indicate the patch density peak points. The green lines within figure h indicates the transition point from 1 to 0 count/m2.

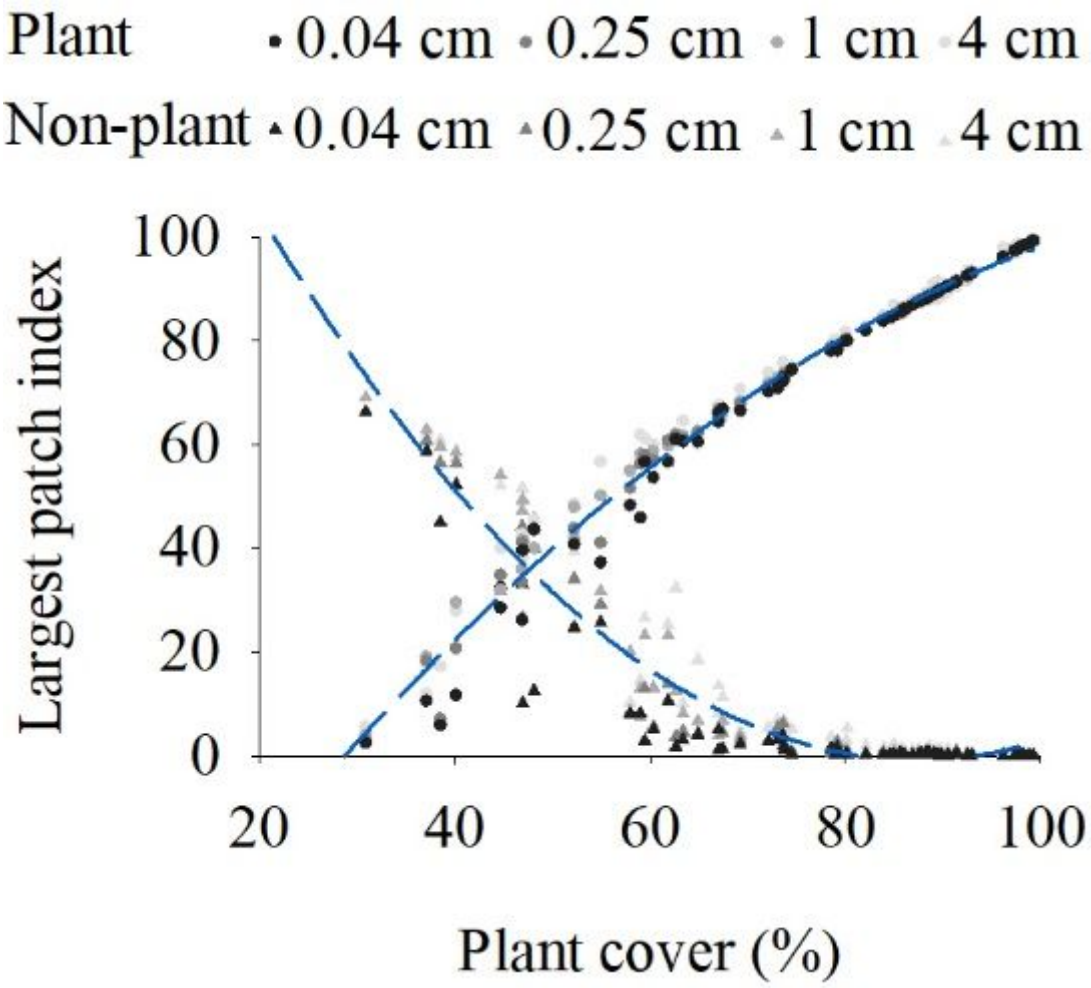

Figure 6

Largest patch index values for plant and non-plant patches under different plant cover levels. The blue fit curves were calculated based on all pixel sizes.

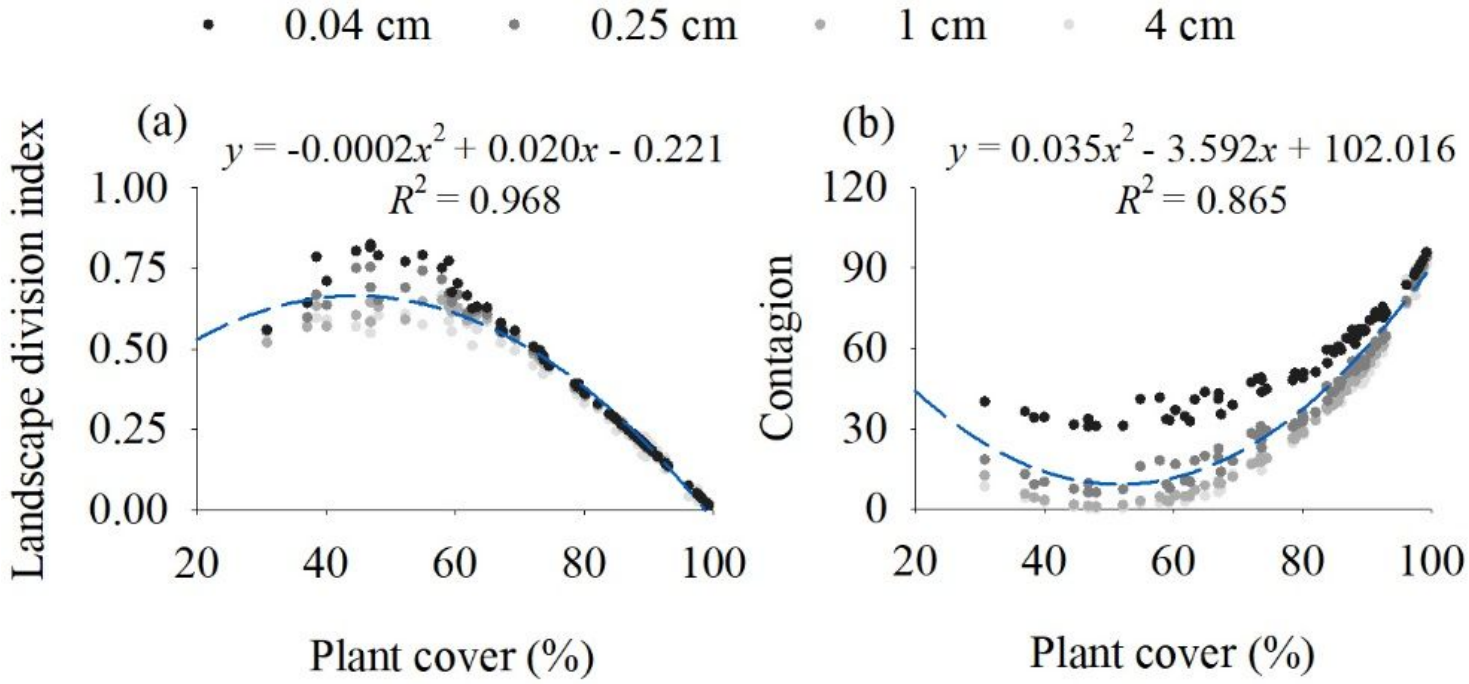

Figure 7

Landscape division index and contagion under different plant covers. The blue fit curves were calculated based on data of all pixel sizes.

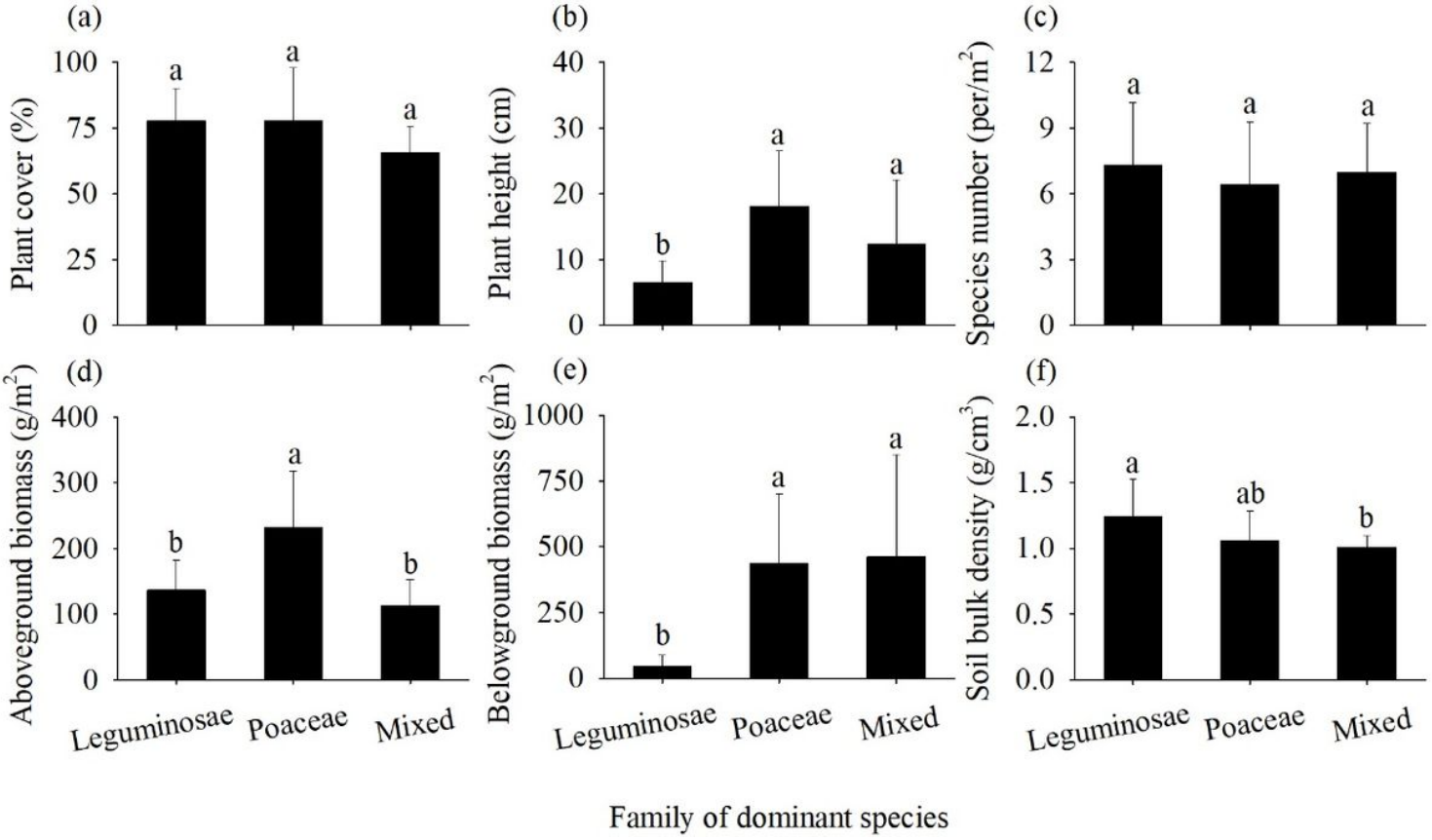

Figure 8

Plant cover, plant height, species number, aboveground biomass, belowground biomass, and soil bulk density for sampling plots dominated by plants of different families. Different letters indicate significant differences at P = 0.05.